IIETA International Information and Engineering Technology Association
Advancing the World of Information and Engineering

Instrumentation Mesure Métrologie
Vol. 25, No. 1, February, 2026, pp. 1-8
Journal homepage: http://iieta.org/journals/i2m

Multi-Band Indoor Path Loss Prediction in Residential Environments

Gregor Alexander Aramice*, Jaafar Qassim Kadhim, Abbas Hussien Miry

Electrical Engineering Department, College of Engineering, Mustansiriyah University, Baghdad 46049, Iraq

Corresponding Author Email: gregoralexander1977@uomustansiriyah.edu.iq

https://doi.org/10.18280/i2m.250101

Received: 5 December 2025
Revised: 23 January 2026
Accepted: 2 February 2026
Available online: 28 February 2026

Keywords:
path loss prediction, multi-wall modeling, residential environment, multi-band frequency, indoor radio communication

ABSTRACT

Residential wireless communication using Wi-Fi is a crucial requirement for various Internet of Things (IoT) applications, including localization and appliance control. Indoor network design requires studying wireless technology radio coverage across various frequency bands. To achieve that, the study utilizes a multi-wall log-distance model for indoor path loss (PL) prediction based on measurement campaigns conducted at 433 MHz, 868 MHz, 2.4 GHz, and 5 GHz bands in a site-specific residential environment. Localized PL exponents and shadowing statistics were derived from measurements collected at twelve selected receiver locations. Findings show that 433 MHz and 868 MHz bands present high distance correlation ($R^2 > 0.92$), while 2.4 GHz and 5 GHz bands suffer from environmental multi-path effects. Compared with free space PL and COST231 benchmarks, the proposed framework minimizes estimation error, achieving a root mean square error (RMSE) ranging from 2.28 dB to 2.50 dB. As a site-specific study, these localized findings offer a precise baseline for optimizing low-power wide-area networks and Wi-Fi deployments in similar environments.

1. INTRODUCTION

Most indoor wireless devices, which operate in the unlicensed Industrial Scientific and Medical (ISM) frequency spectrum and connected to or related to Internet of Things (IoT) concept within these designed wireless networks, require predicting path loss (PL) scenario to decide how the network is to be designed, and how network nodes are distributed and installed to achieve optimal minimum PL and minimal attenuated and more accurate signals [1]. Reliable and high-throughput communication in indoor environments has become increasingly important due to the rise of computing fields, especially with different devices utilized for wireless communications [2]. Optimizing the placement of network nodes is also essential for maximizing network throughput [3].

Network design in indoor environments is challenged by obstructions such as multiple walls, furniture, and even people, which cause greater signal attenuation between the transmitter (Tx) and the receiver (Rx). Confined environments like residential indoor spaces significantly affect radio propagation [4]. PL is a critical factor affecting coverage, reliability, and the lifetime of wireless networks. It is necessary to understand the behavior of PL under line-of-sight (LOS), non-line-of-sight (NLOS) conditions, as well as with/without blockages from walls, doors, and humans, since NLOS signals suffer from the fading problem [1].

Many frequency bands fall under the ISM designation, including 433 MHz, 868 MHz, 2.4 GHz, and 5 GHz. The received signal strength indicator (RSSI) is used as a metric to quantify the power level of the signal received. Due to the complexity of indoor environments, RSSI often exhibits significant loss, resulting in weak communication links [5]. To design a multi-frequency wireless network, it is required to study: a) the coverage area with the best acceptable PL for optimal link performance, b) the distance between Tx and Rx, and c) the number of obstacles (walls, floors, etc.).

Characterizing PL parameters in indoor environments is challenging due to various factors, such as interference, obstacles, and the type of building materials used. Therefore, it is important to consider various empirical PL models that incorporate multi-wall effects. To obtain a reliable prediction model for a new building type (i.e., a new Tx location), additional measurements were performed. PL models, which are mathematical formulas describing link quality between Tx and Rx, play a critical role in the dimensioning and optimization of wireless communication systems [6].

The objective of the study is: (1) to present a PL model applicable to 433 MHz, 868 MHz, 2.4 GHz, and 5 GHz bands in a multi-room residential environment; (2) to perform a walk test to measure network performance based on RSSI values, and (3) to account for the number of walls along the Tx-Rx paths. As a validation of the proposed model, a comparative analysis is conducted against two well-known models, the free space path loss (FSPL) model and the COST231 multi-wall model (MWM), using the root mean square error (RMSE) as the evaluation metric.

2. RELATED WORKS

Many studies concerned PL characteristics and propagation performance in real indoor environments at different

frequency bands. For the 5 GHz frequency, Multi-Wall-and-Floor (MWF) model was utilized to study the effect of walls and floors' penetration characteristics in an indoor environment. It was concluded that wall penetration loss decreases as the number of floors increases [7]. For a 2.4 GHz frequency, a multi-obstruction model was utilized, considering different types of uniform and non-uniform obstructions in an indoor environment to study obstruction penetration loss. The results concluded that the concrete wall has the largest penetration loss [8]. For 2.4/5.3 GHz bands, propagation characteristics investigated using Log-Normal Shadowing (LNS) model in indoor environment through Path Loss Exponent (PLE) and Standard Deviation (STD) parameters, the PLE values ranged between 1.4 and 4.85, it was found that 2.4 GHz band was better than 5 GHz band at NLOS situation, due to Intersymbol Interference (ISI) distortion [9]. For 1.8 GHz, an adjustment to the Motley-Keenan model was proposed with a term considering wall thickness to measure penetration loss at 15, 30, and 4 cm of thickness, and further measuring PL at various distances, as it was concluded that this model is precise and accurate [10]. For the 2.4 – 2.5 GHz band, the Tata indoor PL model proposed for indoor environments, the proposed model considers materials used in Indian building scenarios, and it has suitable extendibility. Also, this model has a closer match to the drive test data compared with other models [11]. For 800 MHz to 6 GHz, log-distance and multi-wall PL models presented in a residential multi-room environment, the Tx antenna height effect was studied, and it was concluded that as height increases, PL decreases. The results concluded that MWM was more accurate [12].

Propagation measurements for both LOS and NLOS conditions were performed in an indoor corridor environment at the 14, 18, and 22 GHz bands. The study considered frequency- and distance-dependent models as well as the angle of arrival (AoA). The results showed that the path loss exponent (PLE) behaves symmetrically around 180° AoA, while better performance is achieved for AoA between 30° and 330°. These findings were attributed to diffraction and waveguide effects in such an environment [13]. For mmWave and sub-Terahertz bands, a unified 3D indoor statistical channel model was proposed for direct and indirect paths, where an exhaustive statistical measurement was conducted using time clusters and the number of sub-paths within each cluster at 28 and 140 GHz [14]. For 5 GHz, Kriging-based interpolation was utilized for PL modeling in an indoor scenario. PL prediction was performed and analyzed, proving that this model has a higher level of confidence over other compared models [15]. At 3.7 GHz and 28 GHz bands, PL prediction studied for staircase at indoor environment, four PL models were tested and exhibited compatibility for average PL, with smaller PL STD obtained from some models than others [16]. For 110, 150, and 170 GHz bands, many PL models were studied and analyzed for both LOS and NLOS cases, the study concluded that mmMAGIC and METIS were the suitable at LOS, while at NLOS, 5GCMDSCIF and METIS models were the best [17]. For 3.7 GHz and 28 GHz, at indoor corridors environment, characteristics of channel propagation studied in LOS and NLOS cases, researchers obtained PLE values between 1.698 and 1.76 in two positions due to reflections from floor and ceiling leading to an interference, and PLE more than 2 at remaining positions, also they concluded that at 28 GHz attenuation of signals increase more than that at 3.7 GHz [18].

3. INDOOR PROPAGATION MODELS

Communication channel may be analyzed by considering radio signal propagation. The characteristics of a radio communication channel are primarily defined by its operating frequency, antenna configurations, and the physical propagation environment [19]. Two distinct PL models were utilized in this section: the LNS model and the MWM. Parameters obtained for these two models due to linear regression between measured PL and targeted variables.

3.1 Log-normal shadowing model

The presence of obstacles within Tx and Rx paths leads to the use of the LNS. PL at a specified distance (d) and in a shadowed environment is given in Eq. (1) [20]:

$$P_L(d) = P_L(d_0) + 10\gamma \log\left(\frac{d}{d_0}\right) + X_\sigma \quad (1)$$

where, $P_L(d)$ represents the mean value of several possible PL(s) for given (d). $P_L(d_0)$ is PL at a close-in distance (d_0) equal to 1 m for indoor environments. γ is the PLE that indicates the amount by which PL increases/decreases with respect to (d). X_σ is a Gaussian variable randomly distributed with zero mean and STD of σ in dB, noting that larger STD leads to an unreliable model with increased uncertainty in PL prediction.

3.2 Multi-wall path loss model

Various types and counts of walls, in addition to other obstacles in residential environments, within Tx and Rx path leads to utilizing the adjusted LNS model with the adjusting term presented in Eq. (2) [12]:

$$P_L(d) = P_L(d_0) + \left(10\gamma \log\left(\frac{d}{d_0}\right)\right) + \left(\sum_{i=1}^{N} k_i L_i\right) + X_\sigma \quad (2)$$

where, N is number of walls, k_i is count of type i walls exist between Tx and Rx, L_i is PL of type i walls exist between Tx and Rx.

In addition, two comparative models are represented below.

3.3 Free space path loss model

The FSPL acts as the theoretical lower level, assuming no obstacles between Tx and Rx.

$$P_{L_{FS}}(d) = 20\log(d) + 20\log(f) + 20\log(\frac{4\pi}{c}) \quad (3)$$

where,

- d: Distance (meters).
- f: Carrier frequency (Hz).
- c: Speed of light ($\approx 3 \times 10^8$ m/s).

3.4 COST231 multi-wall model

The model is more advanced since it added wall accounts and attenuation.

$$P_{L_{COST231}} = P_{L_{FS}}(d) + \sum_{i=1}^{N} k_i L_i \quad (4)$$

where,

- $P_{L_{FS}}(d)$: Free Space PL calculated above.
- k_i: Number of walls of type i penetrated by the direct path.
- L_i: Standardized attenuation loss (dB) for wall type i.

4. POWER LAW EXPONENT AND STANDARD ERROR

In radio frequency transmission environments, power law exponent (PLE) is a component that models the decrease in signal strength at a specific distance from the Tx. Estimating PLE is vital since it serves as a fundamental parameter in modeling signal behavior and improving estimation accuracy for wireless network design [21]. Empirical derivation of the PLE typically requires collecting RSSI samples through different distances and implementing a regression analysis to align the observed data.

Fluctuations in the PLE are regulated by the surroundings, including the transmitted signal, antenna specifications, and multipath fading resulting from obstacles. Table 1 provides a comparison of established PLE benchmarks across different environments.

Table 1. Power law exponent (PLE) benchmarks in different environments [22]

Environment	PLE
Free space	2
Urban	3 – 4
Suburban	2.5 – 3.5
Indoor	1.6 – 2.7
Rural	2 – 3

For a given sample, the PL exponent (γ) is determined using Eq. (5) [20]:

$$\gamma = \frac{RSSI(d_0) - RSSI(d) - X_\sigma}{10\, log_{10}\left(\frac{d}{d_0}\right)} \quad (5)$$

To reduce the error (e) between measured RSSI and calculated RSSI, γ is calculated (for N reading samples) utilizing different methods, the Least Mean Square (LMS) error is one of these methods, and it is expressed in Eq. (6):

$$F(\gamma) = \sum_{i=1}^{N} (e_i)^2 \quad (6)$$

where, $e = \text{measured RSSI} - \text{calculated RSSI}$.

Eq. (6) can be written as in Eq. (7) [23]:

$$F(\gamma) = \sum_{i=1}^{N} \Big(RSSI_i(d_i) - RSSI(d_0) - 10\gamma\, log_{10}\left(\frac{d_i}{d_0}\right)\Big)^2 \quad (7)$$

where, $RSSI_i$ is the i^{th} sample measured RSSI at (d_i).

The standard deviation (σ) between measured and estimated RSSIs provides a reliable prediction of the shadowing component, and it is given in Eq. (8) [23]:

$$\sigma = \sqrt{\frac{F(\gamma)}{N}} = \sqrt{\frac{\sum_{i=1}^{N}(measured\ RSSI - calculated\ RSSI)^2}{N}} \quad (8)$$

5. EXTRACTING PATH LOSS MODEL

The primary objective is to derive a generalized empirical model that describes PL as a function of Tx-Rx separation distance d. The PLE, STD and d_0 parameters describe the PL model statistically. PLE is utilized to calibrate the propagation model, which effectively configure the specific environment under investigation.

A general simplified PL model is obtained in Eq. (9) [20]:

$$P_L(d) = P_t - [\alpha - \beta \log_{10}(d) + \sigma] \quad (9)$$

where,

$$\alpha = RSSI(d_0) + \beta\, log_{10}(d_0) \quad (10)$$

$$\beta = 10\gamma \quad (11)$$

$$\sigma = \begin{cases} 0 & without\ fading \\ > 0 & with\ fading \end{cases} \quad (12)$$

The extracted general simplified PL model in Eq. (9) is dependent on the value of PLE that is calculated depending on the measured RSSI values through a walk test process.

Total PL considering wall penetration loss is given in Eq. (13):

$$P_{LT}(d) = P_L(d) + \sum_{i=1}^{N} k_i L_i \quad (13)$$

where, $P_{LT}(d)$ is the total PL at the separation distance d.

6. INDOOR MEASUREMENT AND DATA FITTING

The measurement campaigns carried out in a multi-room non-empty (wooden furniture, electrical appliances, but no people) residential environment, as shown in Figure 1, with size of 20 m × 5 m × 2.6 m.

Walls with different types and thicknesses are shown in Table 2.

The RSSI gathering method is based on a walk test to record RSSI values within each one of the four bands separately at a time.

At the four bands, the transmit power stated at (20 dBm), the Bandwidth (BW) stated at (BW = 125 kHz), and for the bands 433 MHz and 868 MHz, the Spreading Factor (SF) stated to (SF = 7) and the Coding Rate (CR) stated to (CR = 4/5).

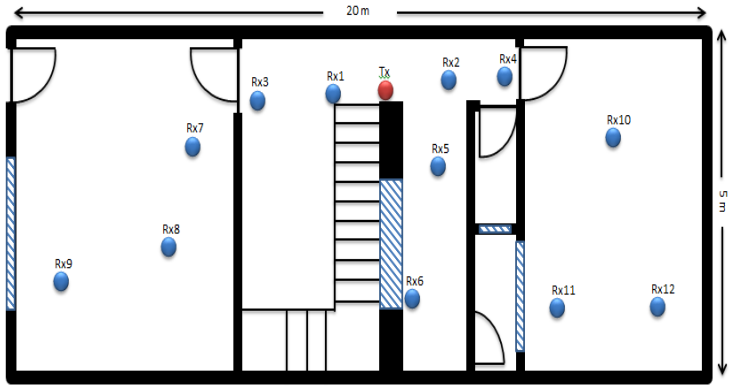

Figure 1. Residential environment floor map with transmitter-receiver (Tx-Rx) locations

Table 2. Diverse wall compositions

Wall Specification	Wall Depth (cm)
Wall with windows	25
Wooden doors	5
Reinforced concrete	30
Load-bearing	25

The measurement system is described as follows:

1. For 2.4 GHz and 5 GHz signals: A TP-Link (Archer C64, AC1200 MU-MIMO Wi-Fi) router serves as the Tx, while an HP (Probook 450 G6) laptop installed with a freeware tool (WifiInfoView v2.97) acts as the Rx to record values of RSSI.
2. For 433 MHz signals: Two transceivers represented by a long-range technology-based Semtech SX1278 module from HELTEC. One module serves as the transmitter, the other as the receiver. Each module is implanted on an Arduino microcontroller. The Tx operates as a standalone unit, while the Rx is connected to the HP (Probook 450 G6) laptop to record values of RSSI.
3. For 868 MHz signals: Two transceivers represented by a long-range 868 MHz module with integrated OLED display and Wi-Fi from HELTEC. One module serves as the transmitter, the other as the receiver. The Tx operates as a standalone unit, while the Rx is connected to the HP (Probook 450 G6) laptop to record values of RSSI.

One position is chosen for the Tx with a 2 m antenna height, which is represented in the center of the tested area that may suffer less obstructions, especially walls; while twelve positions are chosen for the Rx, with 0.7 m antenna height for each. At each Rx position, ten RSSI samples are recorded, and then PL values are calculated.

Table 3. Number of walls between transmitter-receiver (Tx-Rx) paths

Rx Locations	Number of Walls
1	0 (LOS)
2	0 (LOS)
3	0 (LOS)
4	0 (LOS)
5	1 (NLOS)
6	1 (NLOS)
7	1 (NLOS)
8	1 (NLOS)
9	1 (NLOS)
10	2 (NLOS)
11	3 (NLOS)
12	3 (NLOS)

The measuring scenario considers the number of walls in the direct path between the Tx and each Rx as explained in Table 3, which lists the number of walls obstructing each Rx position.

7. RESULTS AND DISCUSSION

At each frequency, 2.4 GHz, 5 GHz, 433 MHz, and 868 MHz, RSSI values were measured for pre-specified distances as shown in Figure 2. At each distance, ten RSSIs are measured, and then the average RSSI is calculated.

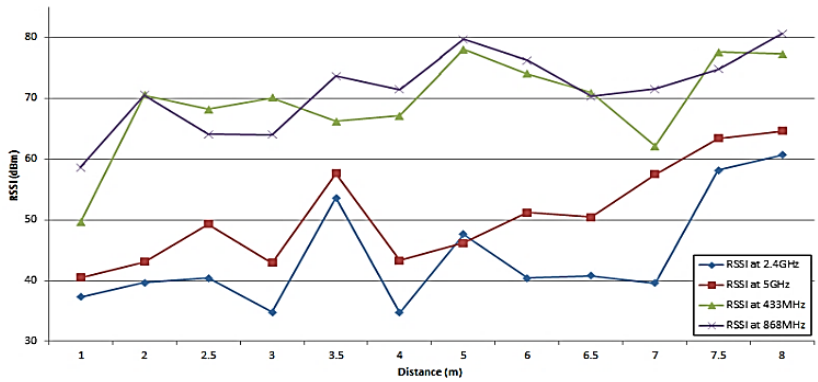

Figure 2. Received signal strength indicator (RSSI) measurement from the walk test

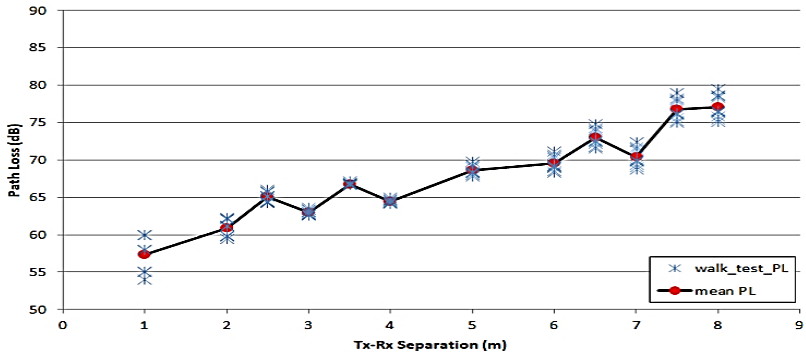

Figure 3. Path loss (PL) at 2.4 GHz

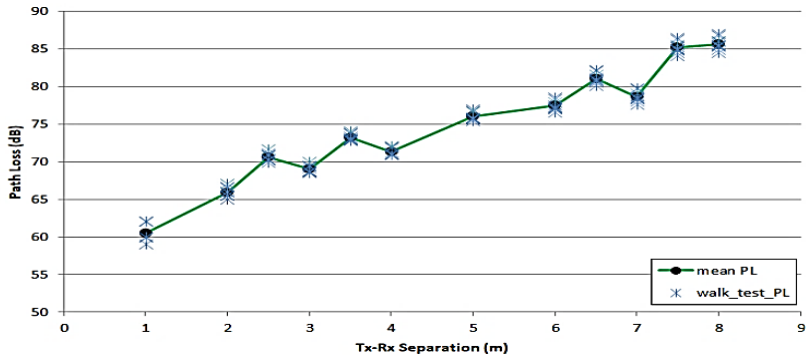

Figure 4. PL at 5 GHz

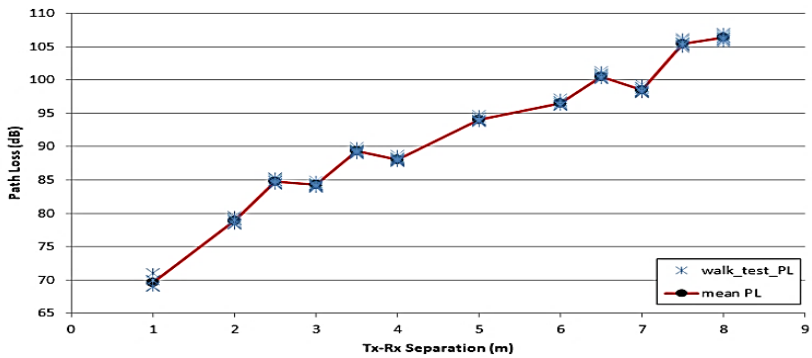

Figure 5. PL at 433 MHz

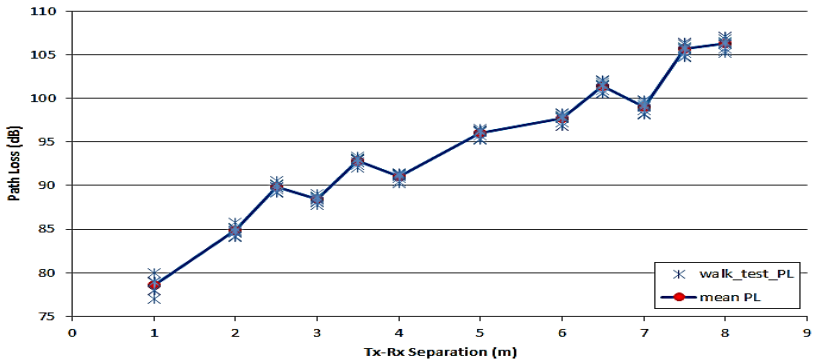

Figure 6. PL at 868 MHz

Figures 3-6 show calculated PL values in (dB) at various Tx-Rx separations in (m) for 2.4 GHz, 5 GHz, 433 MHz, and 868 MHz, respectively.

At each specific distance, the zig-zag pattern indicates the exact change in wall counts.

Figure 7 depicts average PL values for the four frequencies.

The channel parameters obtained in Table 4 via linear least square regression are provided with reliability validation using the determination coefficient (R^2).

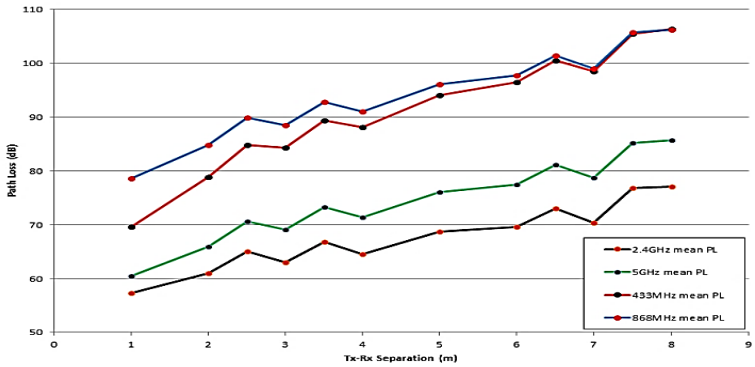

Figure 7. Average PL

Table 4. Channel model parameters

Frequency	$P_L(d_0)$ (dB)	γ	σ (dB)	R^2
2.4 GHz	57.3	1.78	2.50	0.82
5 GHz	60.5	2.38	2.34	0.90
433 MHz	69.6	3.66	2.28	0.95
868 MHz	78.6	2.65	2.31	0.92

From Table 4, the 2.4 GHz band with PLE = 1.78 indicates a normal indoor waveguide effect with clear LOS, while the 5 GHz band with PLE = 2.38 indicates higher loss than the 2.4 GHz band because of high attenuation caused by environmental furniture obstacles. On the other hand, both 433 MHz and 868 MHz reflect characteristics of penetration in this environment due to their long wavelength.

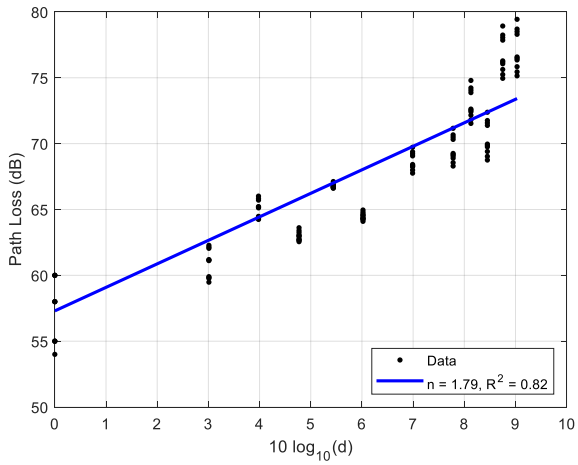

(a)

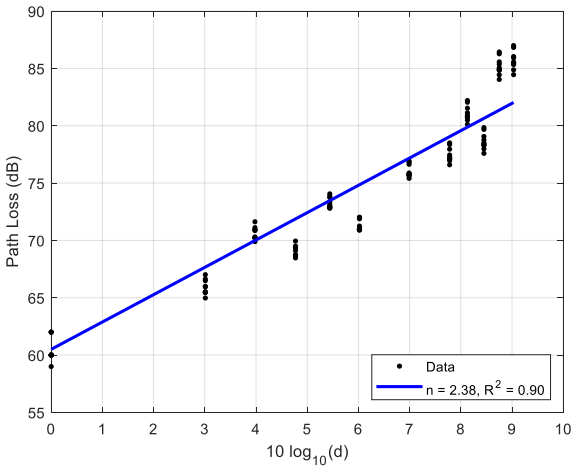

(b)

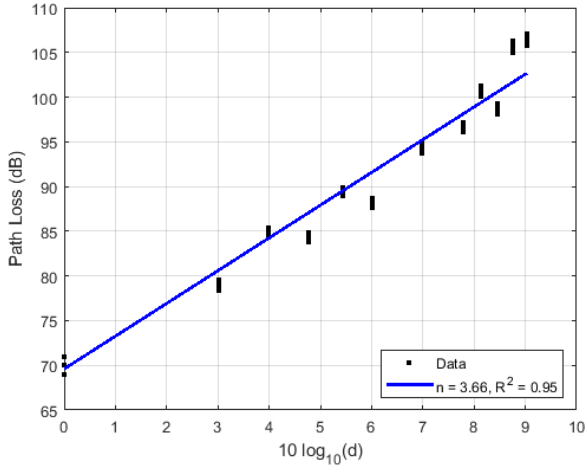

(c)

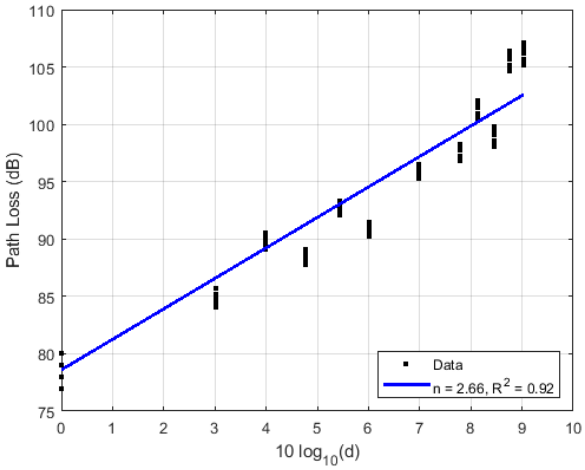

(d)

Figure 8. PL regression analysis for the bands (a) 2.4 GHz, (b) 5 GHz, (c) 433 MHz and (d) 868 MHz

Table 4 also shows that the highest R^2 value (R^2 = 0.95) is observed at 433 MHz, indicating the highest reliability, as 95% of the measured PL is explained at a distance from Tx. This suggests that a small amount of interference is affecting this band in this environment. On the other hand, the R² value at 2.4 GHz is 0.82, reflecting the lowest reliability under these conditions. The 2.4 GHz band is known to be congested and susceptible to multipath fading in indoor environments. Overall, the 433 and 868 MHz bands show the highest modeling reliability.

At the four bands, 2.4 GHz, 5 GHz, 433 MHz, and 868 MHz, a regression analysis for the proposed model is shown in Figure 8.

Figure 9 illustrates PLE versus operating frequency, where in our study, as frequency increases, PLE decreases.

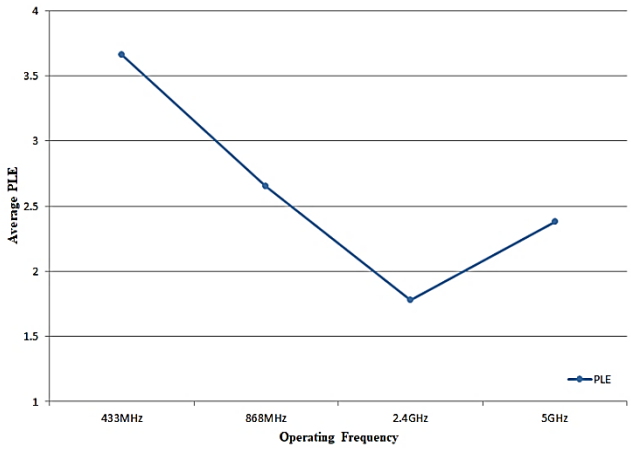

Figure 9. Average power law exponent (PLE) for studied bands

Performance accuracy evaluation of the proposed model, compared against the FSPL and COST231 MWM models, is shown in Table 5, which summarizes the RMSE for all four frequency bands. Eq. (14) defines the RMSE metric formula:

$$RMSE = \sqrt{\frac{1}{N}\sum_{i=1}^{N}\left(P_{L,measured,i} - P_{L,predicted,i}\right)^2} \qquad (14)$$

where,

- N: Total number of measurement points.
- $P_{L,measured,i}$: Actual PL measured at the i^{th} location.
- $P_{L,predicted,i}$: PL value calculated by the proposed empirical model at the same location.

Table 5. RMSE comparison

Frequency	RMSE Proposed	RMSE FSPL	RMSE COST231
2.4 GHz	2.50	15.82	12.43
5 GHz	2.34	16.32	10.08
433 MHz	2.28	54.42	51.54
868 MHz	2.31	51.13	48.03

Note: FSPL = Free Space Path Loss, RMSE = Root Mean Square Error

The results in Table 5 indicate that the proposed model obviously outperforms the generalized models. Where, at 433 MHz, the proposed model achieved an RMSE of 2.28 dB, whereas the FSPL model resulted in an error of 54.42 dB. This variance highlights the importance of site-specific modeling in indoor environments, as architectural attenuation and multipath fading obviously deviate from theoretical free-space conditions.

8. CONCLUSIONS

This study characterized indoor radio propagation in a residential environment at 433 MHz, 868 MHz, 2.4 GHz, and 5 GHz bands. Empirical PL models were established for a multi-room residential environment utilizing LNS and multi-wall considerations to derive a localized PLE and shadow fading statistics (σ). According to the results, as the 433 MHz and 868 MHz bands show high correlation ($R^2 > 0.92$), the 2.4 GHz and 5 GHz bands are sensitive to environmental changes and multipath fading.

It is worth mentioning that, although the empirical model provides an accurate baseline for this specific environment tested, some limitations should be acknowledged. The residential architecture design and the use of 12 Rx locations indicate that these derived parameters are restricted and site-specific for the site under study. For thr future work, a wider variety of indoor environments with different geometries and a larger dataset will be involved to validate this empirical model. But still, this methodology and findings offer a valuable starting point for deploying Wi-Fi and low-power wide-area networks (LPWANs) in similar environments.

ACKNOWLEDGMENT

The authors would like to thank Mustansiriyah University (www.uomustansiriyah.edu.iq) Baghdad – Iraq, for its support in the present work.

REFERENCES

[1] Saleem, A., Zhang, X., Xu, Y., Albalawi, U.A., Younes, O.S. (2023). A critical review on channel modeling: Implementations, challenges and applications. Electronics, 12(9): 2014. https://doi.org/10.3390/electronics12092014

[2] Hussein, N.H., Yaw, C.T., Koh, S.P., Tiong, S.K., Chong, K.H. (2022). A comprehensive survey on vehicular networking: Communications, applications, challenges, and upcoming research directions. IEEE Access, 10: 86127-86180. https://doi.org/10.1109/ACCESS.2022.3198656

[3] Li, Y., Zhu, X., Liao, C., Wang, C.G., Cao, B. (2015). Energy efficiency maximization by jointly optimizing the positions and serving range of relay stations in cellular networks. IEEE Transactions on Vehicular Technology, 64(6): 2551-2560. https://doi.org/10.1109/TVT.2014.2342236

[4] Chrysikos, T., Georgopoulos, G., Kotsopoulos, S. (2011). Attenuation over distance for indoor propagation topologies at 2.4 GHz. In 2011 IEEE Symposium on Computers and Communications (ISCC), Kerkyra, Greece, pp. 329-334. https://doi.org/10.1109/ISCC.2011.5983799

[5] Sesyuk, A., Ioannou, S., Raspopoulos, M. (2022). A survey of 3D indoor localization systems and technologies. Sensors, 22(23): 9380. https://doi.org/10.3390/s22239380

[6] Kongsavat, A., Karupongsiri, C. (2020). Path loss model for smart meter on LoRaWAN technology with unidirectional antenna in an urban area of Thailand. In 2020 IEEE International Conference on Computational Electromagnetics (ICCEM), Singapore, pp. 260-262. https://doi.org/10.1109/ICCEM47450.2020.9219522

[7] Lott, M., Forkel, I. (2021). A multi-wall-and-floor model for indoor radio propagation. In IEEE VTS 53rd

Vehicular Technology Conference, Spring 2001. Proceedings (Cat. No.01CH37202), Rhodes, Greece, pp. 464-468. https://doi.org/10.1109/VETECS.2001.944886
[8] Mohammed, Y.E., Abdallah, A.S., Liu, Y.A. (2003). Characterization of indoor penetration loss at ISM band. In Proceedings of Asia-Pacific Conference on Environmental Electromagnetics, 2003 (CEEM 2003), Hangzhou, China, pp. 25-28. https://doi.org/10.1109/CEEM.2003.238475
[9] Lim, J.W., Shin, Y.S., Yook, J.G. (2004). Experimental performance analysis of IEEE802.11a/b operating at 2.4 and 5.3 GHz. In APCC/MDMC '04. The 2004 Joint Conference of the 10th Asia-Pacific Conference on Communications and the 5th International Symposium on Multi-Dimensional Mobile Communications Proceeding, Beijing, China, pp. 133-136. https://doi.org/10.1109/APCC.2004.1391667
[10] Lima, A.G.M., Menezes, L.F. (2005). Motley-Keenan model adjusted to the thickness of the wall. In SBMO/IEEE MTT-S International Conference on Microwave and Optoelectronics, 2005, Brasilia, Brazil, pp. 180-182. https://doi.org/10.1109/IMOC.2005.1580040
[11] Rath, H.K., Timmadasari, S., Panigrahi, B., Simha, A. (2017). Realistic indoor path loss modeling for regular WiFi operations in India. In 2017 Twenty-third National Conference on Communications (NCC), Chennai, India, pp. 1-6. https://doi.org/10.1109/NCC.2017.8077107
[12] Kacou, M., Guillet, V., El Zein, G., Zaharia, G. (2018). A multi-wall and multi-frequency home environment path loss characterization and modeling. In 12th European Conference on Antennas and Propagation (EuCAP 2018), London, UK, pp. 1-5. https://doi.org/10.1049/cp.2018.0464
[13] Elmezughi, M.K., Afullo, T.J., Oyie, N.O. (2021). Performance study of path loss models at 14, 18, and 22 GHz in an indoor corridor environment for wireless communications. SAIEE Africa Research Journal, 112(1): 32-45. https://doi.org/10.23919/SAIEE.2021.9340535
[14] Ju, S., Xing, Y., Kanhere, O., Rappaport, T.S. (2021). Millimeter wave and sub-terahertz spatial statistical channel model for an indoor office building. IEEE Journal on Selected Areas in Communications, 39(6): 1561-1575. https://doi.org/10.1109/JSAC.2021.3071844
[15] Diago-Mosquera, M.E., Aragón-Zavala, A., Vargas-Rosales, C. (2021). The performance of in-building measurement-based path loss modelling using kriging. IET Microwaves, Antennas & Propagation, 15(12): 1564-1576. https://doi.org/10.1049/mia2.12163
[16] Samad, M.A., Choi, D.Y., Choi, K. (2023). Path loss measurement and modeling of 5G network in emergency indoor stairwell at 3.7 and 28 GHz. PLoS ONE, 18(3): e0282781. https://doi.org/10.1371/journal.pone.0282781
[17] Jazea, N.A., Ali, M.H., Sherif, N.H. (2024). Study and analysis indoor path loss models for low-Terahertz mmWaves. Mathematical Modelling of Engineering Problems, 11(8): 2219-2226. https://doi.org/10.18280/mmep.110823
[18] Diba, F.D., Samad M.A., Choi, D.Y. (2021). Centimeter and millimeter-wave propagation characteristics for indoor corridors: Results from measurements and models. IEEE Access, 9: 158726-158737. https://doi.org/10.1109/ACCESS.2021.3130293
[19] Wu, H.R., Zhang, L.H., Miao, Y.S. (2017). The propagation characteristics of radio frequency signals for wireless sensor networks in large-scale farmland. Wireless Personal Communications, 95(4): 3653-3670. https://doi.org/10.1007/s11277-017-4018-5
[20] Aramice, G.A., Miry, A.H., Salman, T.M. (2023). Optimal long-range-wide-area-network parameters configuration for Internet of Vehicles applications in suburban environments. Journal of Engineering and Sustainable Development, 27(6): 754-770. https://doi.org/10.31272/jeasd.27.6.7
[21] Rademacher, M., Linka, H., Horstmann, T., Henze, M. (2021). Path loss in urban LoRa networks: A large-scale measurement study. In 2021 IEEE 94th Vehicular Technology Conference (VTC2021-Fall), Norman, OK, USA, pp. 1-6. https://doi.org/10.1109/VTC2021-Fall52928.2021.9625531
[22] Rappaport, T.S. (2024). Wireless Communications: Principles and Practice (Second edition). Cambridge University Press. https://doi.org/10.1017/9781009489843
[23] Zakaria, Y.A., Hamad, E.K.I., Elhamid, A.S.A., El-Khatib, K.M. (2021). Developed channel propagation models and path loss measurements for wireless communication systems using regression analysis techniques. Bulletin of the National Research Centre, 45: 54. https://doi.org/10.1186/s42269-021-00509-x

NOMENCLATURE

$P_L(d)$	Mean value of several possible path losses
$P_L(d_0)$	Path loss at a close-in distance (d_0) equal to 1 m

Greek symbols

γ	Path loss exponent
X_σ	Gaussian variable randomly distributed with zero mean
σ	Standard deviation